Multimodal Cortical Parcellation Based on Anatomical and Functional Brain Connectivity

Chendi Wang, Burak Yoldemir, Rafeef Abugharbieh

BiSICL, University of British Columbia, Vancouver, Canada
chendiw@ece.ubc.ca

Abstract. Reliable cortical parcellation is a crucial step in human brain network analysis since incorrect definition of nodes may invalidate the inferences drawn from the network. Cortical parcellation is typically cast as an unsupervised clustering problem on functional magnetic resonance imaging (fMRI) data, which is particularly challenging given the pronounced noise in fMRI acquisitions. This challenge manifests itself in rather inconsistent parcellation maps generated by different methods. To address the need for robust methodologies to parcellate the brain, we propose a multimodal cortical parcellation framework based on fused diffusion MRI (dMRI) and fMRI data analysis. We argue that incorporating anatomical connectivity information into parcellation is beneficial in suppressing spurious correlations commonly observed in fMRI analyses. Our approach adaptively determines the weighting of anatomical and functional connectivity information in a data-driven manner, and incorporates a neighborhood-informed affnity matrix that was recently shown to provide robustness against noise. To validate, we compare parcellations obtained via normalized cuts on unimodal vs. multimodal data from the Human Connectome Project. Results demonstrate that our proposed method better delineates spatially contiguous parcels with higher test-retest reliability and improves inter-subject consistency.

Keywords: Anatomical connectivity, brain network analysis, clustering, functional connectivity, multimodal cortical parcellation

1 Introduction

Brain cortical parcellation refers to subdividing the cerebral cortex into regions that exhibit internal homogeneity in certain properties [1]. Connectivity-based parcellation (CBP) is a promising method for brain cortical parcellation, where voxels in the brain are divided into a coarser collection of functionally or anatomically homogeneous brain regions by clustering voxels with similar connectivity profiles [2]. Among CBP techniques, functional connectivity (FC) based parcellation is the predominant approach, where voxels are grouped according to the statistical dependencies between their functional magnetic resonance imaging (fMRI) time courses [1]. However, even with advanced clustering methods, reliable brain parcellation remains challenging due to the notoriously low signal-to-noise ratio (SNR) of fMRI data. Given the close relationship between anatomical

connectivity (AC) and FC in the brain [3], we argue that simultaneous analysis of AC and FC information for CBP is beneficial. Despite its promising potential, multimodal CBP remains a relatively unexplored direction. To the best of our knowledge, the only existing approach to multimodal CBP uses the overlap among probabilistic parcellation maps derived from different modalities to generate a consensus map [4,5]. A major disadvantage of this approach is its late fusion, i.e the unimodal parcellation is performed in isolation on each modality then combined in a subsequent fusion step rather than jointly analyzing multimodal data in a truly unified framework.

In this paper, we propose a multimodal CBP method where AC and FC, inferred through diffusion MRI (dMRI) and fMRI, are combined. To prevent bias towards any particular task, we use resting state fMRI (RS-fMRI) data, which captures the intrinsic functional brain connectivity. Our rationale in combining AC and FC is that FC estimates tend to contain many false positive correlations due to structured noise arising from confounds such as head movements and cardiac pulsations, whereas AC estimates tend to contain false negatives mainly due to the crossing fiber problem during tractography. Combining both data should thus help alleviate the problems linked to individual modalities. To fuse AC and FC, we use a data-driven adaptive weighting scheme that is based on the reliability of local FC information. To encode AC and FC information, we use a neighborhood-information-embedded multiple density (NMD) affinity matrix which has been recently shown to facilitate adaptive adjustment of voxel affinity values and provide robustness against noise [6].

To evaluate our proposed approach, we use the real data obtained from the Human Connectome Project (HCP) [7]. We apply our approach on normalized cuts (Ncuts) [8] and Ward clustering which are two of the most popular clustering methods for parcellation [1]. We demonstrate the benefits of incorporating AC information by comparing unimodal FC-based vs. multimodal parcellation. We show that our multimodal method achieves higher test-retest reliability and increases inter-subject consistency compared to unimodal parcellation. Further, we qualitatively illustrate that subject-specific parcellation maps better resemble the group parcellation maps when the multimodal approach is used.

2 Materials

In this work, we used the publicly available multimodal HCP Q2 dataset [7]. Along with other imaging modalities, this dataset comprises dMRI and RS-fMRI scans of 38 subjects with no history of neurological disease (17 males and 21 females, ages ranging from 22 to 35).

2.1 RS-fMRI Data

The RS-fMRI data comprised two sessions, each having a 30 minute acquisition with a TR of 0.72 s and an isotropic voxel size of 2 mm. Preprocessing already applied to the data by HCP [9] included gradient distortion correction,

motion correction, spatial normalization to MNI space, and intensity normalization. Additionally, we regressed out motion artifacts, mean white matter and cerebrospinal fluid signals, and principal components of high variance voxels. Next, we applied a bandpass filter with cutoff frequencies of 0.01 and 0.1 Hz to minimize the effects of low frequency drift and high frequency noise. The data were finally demeaned and normalized by the standard deviation.

2.2 dMRI Data

The dMRI data had an isotropic voxel size of 1.25 mm, three shells (b=1000, 2000 and 3000 s/mm^2) and 288 gradient directions with six b=0 images. The data, which have already been corrected for EPI distortion, eddy current, gradient nonlinearity and motion artifacts by HCP [9], were downsampled to 2 mm isotropic resolution to reduce the computational cost.

3 Methods

Our approach starts by estimating the AC and FC from dMRI and fMRI data, respectively, in Section 3.1. Subsequently, we construct our multimodal connectivity model by fusing anatomical and functional connectivity information into a single connectivity metric in Section 3.2. We provide an overview of how we encode our connectivity metric into a neighborhood-informed affinity matrix in Section 3.3, on which parcellation is finally performed using clustering method.

3.1 Estimating Brain Connectivity

AC Estimation: We perform whole-brain deterministic global tractography on dMRI data using MITK [10] to reconstruct all fiber tracts in the brain simultaneously, which alleviates error propagation along tracts. Given the tracts, we define an AC fingerprint for each voxel [11] as the number of tracts connecting that voxel to each target region. Target regions can be taken as every other voxel, or parcels from an initial parcellation map. Since the human brain has a sparse AC structure, we opt to use the 116 regions in the Automated Anatomical Labeling (AAL) atlas as target regions instead of using individual voxels. This reduces the number of unknowns to be estimated, i.e. elements of AC fingerprints, from more than 100,000 to 116 per voxel, resulting in more robust AC estimates in addition to reducing computational complexity. Finally, our AC estimate is defined as the cross-correlation between the computed AC fingerprints of voxels of interest. Depending on the application, voxels of interest can be defined as the voxels in the whole brain or specific regions.

FC Estimation: Let $\mathbf{Z}$ be a $t \times N$ matrix of preprocessed fMRI time courses, where t is the number of time points and N is the number of voxels of interest. We estimate the FC matrix using Pearson's correlation: $\mathbf{FC} = \mathbf{Z}^T\mathbf{Z}/(t-1)$. Although the interpretation of negative correlations is currently an open research problem, there is a lack of anatomical evidence for negative correlations unlike positive correlations [12]. We thus set negative values in the FC matrix to zero.

3.2 Adaptively Weighted Multimodal Connectivity Model

To reduce false positive correlations in FC estimates and false negatives in AC estimates, we propose a multimodal CBP model that we later demonstrate to outperform the unimodal approach.

Multimodal Connectivity Model: To generate our multimodal connectivity matrix **MC**, we deploy the following linearly weighted model:

$$\mathbf{MC}_{ij} = \rho_{ij}\mathbf{FC}_{ij} + (1 - \rho_{ij})\mathbf{AC}_{ij}, \tag{1}$$

where $\mathbf{AC}_{ij}$ and $\mathbf{FC}_{ij}$ are estimates of AC and FC between voxels i and j, and ρ_{ij} is the relative weighting term.

Normalization: It is important to note that naive combination of AC and FC values may not be suitable since their distributions are largely divergent. FC distribution has a mean value of 0.2564 as empirically estimated from a group of 38 healthy subjects, while AC distribution has a mean value of 0.7295. The difference in their distribution makes a single value in two distributions represent different measures of connectivity, leading to misleading combined correlation value. To compensate for this, we map the AC values to match the FC distribution using histogram matching as follows. Let $a_1 \leq a_2, \ldots, \leq a_M$ be the raw AC data, and $f_1 \leq f_2, \ldots, \leq f_M$ be the FC values, where M is the number of voxel pairs. We compute the histograms of AC and FC, followed by their cumulative distribution functions $F_a(x) = P(X \leq x), x \in [a_1, a_M]$ and $F_f(y) = P(Y \leq y), y \in [f_1, f_M]$. $P(X \leq x)$ is the probability that the random variable X takes on a value less than or equal to x. Next, we replace each AC value a_i with the FC value f_j which satisfies $F_a(a_i) = F_f(f_j)$. This normalization enables unbiased multimodal AC and FC data fusion, where each AC value after normalization is used in the multimodal connectivity model in (1).

Adaptive Weighting: To set the relative weighting term ρ_{ij} in (1) in a data-driven manner, we construct a measure of local reliability in fMRI observations. The idea is to weigh down the effect of FC in voxels where fMRI observations are deemed to be unreliable. We estimate a reliability metric γ_i for a given voxel i as the cross-correlation of its local FC fingerprints estimated from the first and second halves (indicated as **FC1** and **FC2**) of its time points. The local FC fingerprint of voxel i refers to the FC profiles within its neighborhood δ_i, i.e. $\{\mathbf{FC}_{ik}\}$, $\forall k, k \in \delta_i$. Presumably, the local FC fingerprint of a voxel should be similar in two different time windows in the absence of an explicit task and noise. The reliability values γ_i will be low for voxels where noise in fMRI time courses is more pronounced, and more weight will be assigned to AC. This metric can be mathematically expressed as:

$$\gamma_i = \frac{n_{\delta_i} \sum\limits_{k \in \delta_i} \mathbf{FC1}_{ik}\mathbf{FC2}_{ik} - \sum\limits_{k \in \delta_i} \mathbf{FC1}_{ik} \sum\limits_{k \in \delta_i} \mathbf{FC2}_{ik}}{\sqrt{n_{\delta_i} \sum\limits_{k \in \delta_i} \mathbf{FC1}_{ik}^2 - (\sum\limits_{k \in \delta_i} \mathbf{FC1}_{ik})^2}\sqrt{n_{\delta_i} \sum\limits_{k \in \delta_i} \mathbf{FC2}_{ik}^2 - (\sum\limits_{k \in \delta_i} \mathbf{FC2}_{ik})^2}} \tag{2}$$

where n_{δ_i} is the number of neighbors of voxel i. We set δ_i to be the 26 nearest neighborhood of voxel i. We use the information from the immediate neighbors of a given voxel, as it has been shown that larger neighborhoods might make the analysis more prone to acquisition and registration artifacts [3]. The reliability of a functional connection, ρ_{ij}, is implicitly bounded by the voxel $v, v \in \{i, j\}$, having relatively lower reliability. As such, we define ρ_{ij} as the minimum reliability of voxels i and j as shown in (3).

$$\rho_{ij} = min(\gamma_i, \gamma_j) \tag{3}$$

3.3 Affinity Matrix Estimation

Traditionally, correlations or distances are mapped using a Gaussian kernel to produce an affinity matrix for clustering. However, this entails an inherent assumption of fixed density distribution of affinity values, which rarely holds true in practice. We thus adopt the NMD affinity matrix [6], which embeds local neighborhood information into the affinity matrix and adaptively tunes the density distribution of affinity values. The NMD affinity matrix is defined as:

$$\mathbf{A}_{ij}^{\mathbf{MC}} = \exp(-\frac{K_i K_j d_{ij}^2}{\overline{d_i}\,\overline{d_j}}), \tag{4}$$

where d_{ij} is the distance between voxels i and j defined as $1 - \mathbf{MC}_{ij}$, $\overline{d_i}$ is the average distance between voxel i and the one fourth of its nearest neighbors [6], and K_i is a measure of the spread of $\{d_i\}$, the set of distance values from voxel i to all of its neighbors as we proposed in [6]. This formulation effectively modifies the $\mathbf{A}_{ij}$ values based on putative cluster memberships of voxels i and j. Specifically, it scales the affinity value down when i and j are likely to be in different clusters since the spread of $\{d_i\}$ and $\{d_j\}$ would presumably be large, resulting in a large $K_i K_j$. The opposite holds true when voxels i and j are likely to be in the same cluster. $\mathbf{A}_{ij}^{\mathbf{FC}}$ values for unimodal parcellation can be generated by defining d_{ij} in (4) as $1 - \mathbf{FC}_{ij}$.

In our experiments, we use $\mathbf{A}_{ij}^{\mathbf{FC}}$ and $\mathbf{A}_{ij}^{\mathbf{MC}}$ as the inputs to clustering methods for unimodal and multimodal parcellation, respectively. We highlight that the estimation of multimodal connectivity model and affinity matrices are independent of the clustering method chosen and they can be used in conjunction with any clustering algorithm that takes an affinity matrix as its input. Similar results have been observed using Ward clustering, however we only show the results obtained using Ncuts due to the space limitations.

4 Results and Discussion

In this work, we focused on parcellating the inferior parietal lobule (IPL) and the visual cortex (VC), both known to possess functional and anatomical heterogeneity [13,14]. The voxels of interest are thus taken to be the voxels within

the IPL and VC from the left hemisphere in the AAL atlas. In the HCP dataset, dMRI data are in the native diffusion space of each subject whereas fMRI data are in the standard MNI space. To fuse AC and FC in a common space, we warped the fractional anisotropy image of each subject to the MNI space using affine registration. The resulting transformation was then used to map the AC matrices of each individual subject to the MNI space using nearest neighbor interpolation.

Cortical parcellation maps are challenging to validate due to the lack of ground truth. However, assuming there truly is a functional parcellation, it should presumably remain stable for each subject and consistent across subjects. Thus, we base our quantitative validation on intra-subject stability and inter-subject consistency of the resulting brain parcels, which we measure using Dice similarity coefficient after relabeling parcels using the Hungarian algorithm [15]. Further, we qualitatively evaluate our method by visually comparing the group parcellation map with those estimated from individual subjects. Our rationale here is that the group map is expected to be more reliable since it is generated by pooling data across subjects, effectively increasing the SNR. It can thus be used as pseudo ground truth to compare individual parcellation maps against. As common in literatures [13,14], we divided the IPL into six and the VC into nine subregions in our experiments.

4.1 Quantitative Results

Intra-Subject Test-Retest Reliability: To evaluate the intra-subject test-retest reliability of our proposed approach, we calculated the subject-specific parcellation maps from the two RS-fMRI sessions of each subject separately. We then compared the resulting two parcellation maps for each subject and averaged the results across subjects. In the IPL, our proposed multimodal CBP method improved the test-retest reliability from 0.92 ± 0.09 to 0.94 ± 0.08 compared to unimodal parcellation. In the VC, our method increased the average Dice coefficient from 0.88 ± 0.08 to 0.90 ± 0.08. The difference between the two techniques are statistically significant for both regions at $p < 0.05$ based on the Wilcoxon signed rank test, which was also used in inter-subject validation.

Inter-Subject Consistency: We adopted the leave-one-out cross-validation approach to assess inter-subject consistency. Taking one subject at a time, we compared the group parcellation map obtained using the remaining subjects with the subject-specific parcellation map. For generating group parcellation maps, we first concatenated the voxel time courses temporally across scans and S=38 subjects. Group FC matrices were then computed using the pooled time courses, and group AC matrices were generated by averaging AC matrices from S-1 subjects prior to applying Ncuts. In the IPL, using multimodal parcellation instead of unimodal improved the Dice coefficient from 0.85 ± 0.1 to 0.89 ± 0.1. In the VC, Dice coefficient improved from 0.85 ± 0.1 to 0.88 ± 0.09. For both regions, the difference is statistically significant at $p < 0.05$.

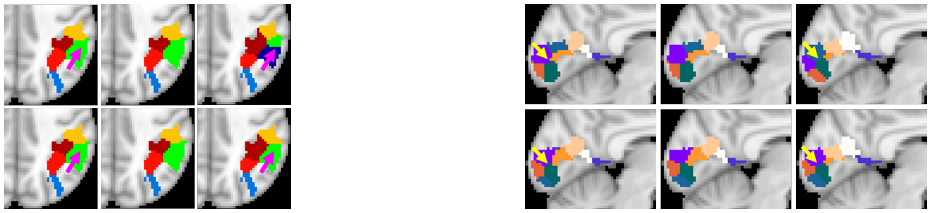

Fig. 1: Qualitative results for the IPL (left) and the VC (right) using the HCP data. For each region, top row shows the results of FC-based parcellation, and bottom row shows the results of the proposed multimodal parcellation. 1st column: Group maps, 2nd and 3rd columns: The subject-specific maps with the highest and lowest Dice coefficient with the group maps. The significant differences are highlighted with arrows.

4.2 Qualitative Results

To qualitatively evaluate the reliability of our proposed method, we generated a group parcellation map using the group affinity matrix of all subjects, and compared it with subject-specific parcellation maps. For brevity, we only present subjects showing the highest and lowest similarity with the group map indicated by Dice coefficient in Fig. 1. The group maps obtained using FC-based unimodal parcellation and the proposed multimodal CBP did not exhibit major differences indicating that using unimodal parcellation suffices when there is enough data. However, the subject-specific map having the lowest Dice coefficient (top right) shows major differences compared to the group map (top left) when the unimodal method is used. It can be observed that there are differences in the number of parcels and the parcel boundaries on the slices shown. In contrast, more reliable results can be obtained using our proposed multimodal method. Taken collectively, our results indicate that incorporating AC information into parcellation can increase the robustness of the analysis, resulting in more reproducible parcels both among different scans of the same subject and across different subjects.

5 Conclusions

We proposed a multimodal approach to cortical parcellation based on joint analysis of anatomical and functional brain connectivity. Our method determines the weighting between AC and FC in a data-driven manner, by adaptively assigning higher weight to AC at voxels where FC is deemed less reliable. On real data from 38 healthy subjects, we quantitatively demonstrated the potential of our method compared to FC-based unimodal parcellation in terms of test-retest reliability and inter-subject consistency. Qualitatively, we showed that subject-specific parcellations better resemble the group maps using our multimodal CBP model. We thus argue that multimodal parcellation may enable more reliable identification of brain regions leading to potentially more accurate higher-level brain network analyses. Our future work will focus on the metric learning for the fusion method, and the application of our method to whole-brain parcellation.

References

1. Thirion, B., Varoquaux, G., Dohmatob, E., Poline, J.B.: Which fmri clustering gives good brain parcellations? Frontiers in neuroscience **8** (2014)
2. de Reus, M.A., Van den Heuvel, M.P.: The parcellation-based connectome: limitations and extensions. Neuroimage **80** (2013) 397–404
3. Honey, C., Sporns, O., Cammoun, L., Gigandet, X., Thiran, J.P., Meuli, R., Hagmann, P.: Predicting human resting-state functional connectivity from structural connectivity. Proceedings of the National Academy of Sciences **106**(6) (2009) 2035–2040
4. Wang, J., Yang, Y., Fan, L., Xu, J., Li, C., Liu, Y., Fox, P.T., Eickhoff, S.B., Yu, C., Jiang, T.: Convergent functional architecture of the superior parietal lobule unraveled with multimodal neuroimaging approaches. Human brain mapping **36**(1) (2015) 238–257
5. Zhang, D., Snyder, A.Z., Shimony, J.S., Fox, M.D., Raichle, M.E.: Noninvasive functional and structural connectivity mapping of the human thalamocortical system. Cerebral cortex **20**(5) (2010) 1187–1194
6. Wang, C., Yoldemir, B., Abugharbieh, R.: Improved functional cortical parcellation using a neighborhood-information-embedded affinity matrix. In: IEEE International Symposium on Biomedical Imaging, IEEE Press (2015) 1340–1343
7. Van Essen, D.C., Smith, S.M., Barch, D.M., Behrens, T.E., Yacoub, E., Ugurbil, K., Consortium, W.M.H., et al.: The wu-minn human connectome project: an overview. Neuroimage **80** (2013) 62–79
8. Craddock, R.C., James, G.A., Holtzheimer, P.E., Hu, X.P., Mayberg, H.S.: A whole brain fmri atlas generated via spatially constrained spectral clustering. Human brain mapping **33**(8) (2012) 1914–1928
9. Glasser, M.F., Sotiropoulos, S.N., Wilson, J.A., Coalson, T.S., Fischl, B., Andersson, J.L., Xu, J., Jbabdi, S., Webster, M., Polimeni, J.R., et al.: The minimal preprocessing pipelines for the human connectome project. Neuroimage **80** (2013) 105–124
10. Neher, P.F., Stieltjes, B., Reisert, M., Reicht, I., Meinzer, H.P., Fritzsche, K.H.: Mitk global tractography. In: SPIE medical imaging, International Society for Optics and Photonics (2012) 83144D–83144D
11. Johansen-Berg, H., Behrens, T., Robson, M., Drobnjak, I., Rushworth, M., Brady, J., Smith, S., Higham, D., Matthews, P.: Changes in connectivity profiles define functionally distinct regions in human medial frontal cortex. Proceedings of the National Academy of Sciences of the United States of America **101**(36) (2004) 13335–13340
12. Skudlarski, P., Jagannathan, K., Calhoun, V.D., Hampson, M., Skudlarska, B.A., Pearlson, G.: Measuring brain connectivity: diffusion tensor imaging validates resting state temporal correlations. Neuroimage **43**(3) (2008) 554–561
13. Wang, J., Fan, L., Zhang, Y., Liu, Y., Jiang, D., Zhang, Y., Yu, C., Jiang, T.: Tractography-based parcellation of the human left inferior parietal lobule. Neuroimage **63**(2) (2012) 641–652
14. Montaser-Kouhsari, L., Landy, M.S., Heeger, D.J., Larsson, J.: Orientation-selective adaptation to illusory contours in human visual cortex. The Journal of neuroscience **27**(9) (2007) 2186–2195
15. Munkres, J.: Algorithms for the assignment and transportation problems. Journal of the Society for Industrial & Applied Mathematics **5**(1) (1957) 32–38